Protein adsorption on and swelling of polyelectrolyte brushes: A simultaneous ellipsometry-quartz crystal microbalance study

Eva Bittrich
Leibniz Institute of Polymer Research Dresden, Hohe Str. 6, 1069 Dresden, Germany

Keith Brian Rodenhausen
Department of Chemical and Biomolecular Engineering, 207 Othmer Hall, University of Nebraska–Lincoln, Lincoln, Nebraska 68588-0643

Klaus-Jochen Eichhorn[a)]
Leibniz Institute of Polymer Research Dresden, Hohe Str. 6, 1069 Dresden, Germany

Tino Hofmann and Mathias Schubert
Department of Electrical Engineering, University of Nebraska–Lincoln, 209N Scott Engineering Center, P.O. Box 880511, Lincoln, Nebraska 68588-0511

Manfred Stamm and Petra Uhlmann[b)]
Leibniz Institute of Polymer Research Dresden, Hohe Str. 6, 1069 Dresden, Germany

(Received 28 October 2010; accepted 2 December 2010; published 10 January 2011)

With a coupled spectroscopic ellipsometry-quartz crystal microbalance with dissipation (QCM-D) experimental setup, quantitative information can be obtained about the amount of buffer components (water molecules and ions) coupled to a poly(acrylic acid) (PAA) brush surface in swelling and protein adsorption processes. PAA Guiselin brushes with more than one anchoring point per single polymer chain were prepared. For the swollen brushes a high amount of buffer was found to be coupled to the brush-solution interface in addition to the content of buffer inside the brush layer. Upon adsorption of bovine serum albumin the further incorporation of buffer molecules into the protein-brush layer was monitored at overall electrostatic attractive conditions [below the protein isolectric poimt (IEP)] and electrostatic repulsive conditions (above the protein IEP), and the shear viscosity of the combined polymer-protein layer was evaluated from QCM-D data. For adsorption at the "wrong side" of the IEP an incorporation of excess buffer molecules was observed, indicating an adjustment of charges in the combined polymer-protein layer. Desorption of protein at *p*H 7.6 led to a very high stretching of the polymer-protein layer with additional incorporation of high amounts of buffer, reflecting the increase of negative charges on the protein molecules at this elevated *p*H. © *2010 American Vacuum Society.* [DOI: 10.1116/1.3530841]

I. INTRODUCTION

For the development of smart surfaces high attention is focused on stimuli-responsive polymers.[1,2] Especially highly swellable polymer brushes, with the polymer chains grafted chemically to the surface, are promising because properties like the surface wettability or charge interactions can be switched over a wide range according to changes in the environmental conditions: *p*H, salt concentration, or temperature.[3–7]

Among the field of polyelectrolyte brushes the swelling behavior of weak polyanionic brushes consisting of poly(acrylic acid) (PAA) is well investigated.[8–11] These polymer brushes are characterized by their *p*H dependent deprotonation of COOH-groups along the chains to negatively charged COO^- groups, as well as their nonmonotonic dependence of the swollen brush thickness on the ionic strength of the solution.[8,9] In the osmotic regime an increase of the ionic strength of the solution is considered to lead to an increase of counterion condensation inside the brush. Thus, the polymer chains expand due to the osmotic pressure of localized counterions.[12,13] With further increasing ionic strength and decreasing Debye screening length in solution, the brush enters the salted regime and collapses.

Regarding the adsorption behavior of the proteins bovine serum albumin (BSA) and human serum albumin (HSA) toward these PAA brushes, the adsorption maximum was found near the IEP of the protein, and adsorption could be observed for likewise negative net charges on brush and protein at the wrong side of the IEP of the protein.[14–18] Also the penetration of protein molecules inside the brush layer could be demonstrated.[14] Two possible explanations exist for the occurrence of adsorption at overall electrostatic repulsive conditions: on one hand, the possibility of charge regulation/reversal on the protein is discussed in terms of an adjustment of the charge of weakly charged amino acids due to the local electrostatic potential inside the polyelectrolyte brush;[18] and, on the other hand, due to a charge anisotropy (patchiness) of the protein, positive charged patches exist on the protein that can lead to an entropically favorable replacement of the small counterions inside the brush by protein molecules.[19]

With optical techniques like *in situ* ellipsometry or *in situ*

a)Electronic mail: kjeich@ipfdd.de
b)Electronic mail: uhlmannp@ipfdd.de

reflectometry, the swelling behavior of thin polymer brushes was investigated, focusing on changes in film thickness and refractive index.[8,17,20] Additionally, protein adsorption processes at solid surfaces or at thin polymer films are commonly examined with these methods,[21,22] and the adsorbed amount of protein is derived according to the approach of De Feijter *et al.*[23]

The adsorbed amount of a surface layer can also be obtained by quartz crystal microbalance with dissipation (QCM-D) measurements, and viscoelastic as well as rigid layers can be investigated.[24–27] With the help of QCM-D, for example, the grafting of polystyrene brushes as well as temperature and *p*H-sensitive swelling of copolymer films was monitored.[28,29] As another example, adsorption of the enzyme tyrosinase to polyelectrolyte surface layers and its remaining activity in the immobilized state were observed.[30]

By combining spectroscopic ellipsometry (SE) and QCM-D it is possible to derive the solvent-content of very thin adsorbed surface layers, leading to a further insight into swelling and adsorption mechanisms.[31,32] Furthermore, for swollen polymer films, like polystyrene brushes in cyclohexane[33] and polyelectrolyte multilayers in aqueous solution,[34] higher acoustical thicknesses (QCM) than optical thicknesses (ellipsometry) could be observed, which was discussed as partly due to the higher acoustic contrast of the QCM.[33] With the latter technique solvent molecules at the film-solution interface can be detected, which couple to the substrate vibration. Thus, the acoustic thickness (QCM) is closer to the hydrodynamic thickness than the optical thickness determined by ellipsometry.[33]

In this article we focus on polymer Guiselin brushes consisting of the weak polyelectrolyte PAA, grafted by an average value of two grafting points per chain.[11,35] Guiselin brushes present an easy means to prepare surface coatings, where the degree of swelling can be controlled via the average number of grafting points per chain governed solely by the grafting temperature. For this special type of polyelectrolyte brush the *p*H-sensitive dissociation behavior, ion distribution, and swelling behavior were reported previously, and the same qualitative swelling behavior as for end-grafted PAA brushes could be found.[35] Also the *p*H-sensitive adsorption of HSA showed the same trend as found for end-grafted brushes.[36]

Swelling of the Guiselin brushes at *p*H 6 for two selected ionic strengths of the solution and adsorption of BSA onto the brushes above and below the protein IEP are monitored with a combinatorial SE–QCM-D setup as a novel hybrid technique to study solid-liquid interfaces. We focus on changes in the amount of viscoelastically coupled buffer (water) molecules to polymer and combined polymer-protein layers.

II. EXPERIMENT

A. Materials

PAA (M_n=26 500 g/mol, M_w/M_n=1.12) and the adhesion promoter poly(glycidyl methacrylate) (PGMA) (M_n =17 500 g/mol, M_w/M_n=1.7) were purchased from Polymer Source, Inc. (Canada). Chloroform and absolute ethanol for the preparation of polymer solutions and extraction of unbound polymer from the surface as well as the protein bovine serum albumin (A6003, defatted) for adsorption studies were purchased from Sigma-Aldrich, Inc. (St. Louis, MO, USA).

For the preparation of 1 and 100 mM phosphate buffer solutions, sodium phosphate monobasic dihydrate and sodium phosphate dibasic dihydrate were purchased from Sigma-Aldrich, Inc., as well. The refractive index $n(\lambda)$ of all buffer solutions was measured with a digital multiple wavelength refractometer DSR-lambda (Schmidt+Haensch GmbH u. Co.) at eight different wavelengths from 435.8 to 706.5 nm. 0.3-mm-thick AT-quartz crystals coated with a 100-nm-thick gold layer (QSX 301, Q-Sense, Frölunda, Sweden) with a resonance frequency at 4.95 ± 0.05 MHz were used as substrates.

B. Polymer film preparation

The Au-coated crystals were used as received from Q-Sense. A 0.02 wt % solution of PGMA in chloroform was spin-coated (2000 rpm, 1000 rpm/s, 10 s) on the Au-coated crystal and annealed under vacuum at 100 °C for 20 min to crosslink PGMA, thus forming an anchoring layer of 2.0 ± 0.5 nm thickness equipped with remaining epoxy groups for the following "grafting-to" process. PAA was spin-coated (1% in ethanol, 2000 rpm, 1000 rpm/s, 20 s) onto the PGMA layer and was annealed at 80 °C under vacuum for 30 min to react remaining epoxy groups of the PGMA with COOH-groups along the chain of PAA, grafting the PAA chains in loops and tails via ester bonds. The annealing temperature was chosen below the glass transition temperature at 105 °C of the polymer to minimize the amount of grafting points and achieve highly swellable polymer brush films. The ungrafted PAA was removed by extraction in 96% ethanol, and the thickness of the grafted PAA layers was measured with SE to be 5.3 ± 0.5 nm.

C. Characterization methods and course of experiments

1. Spectroscopic ellipsometry

Ellipsometric measurements are sensitive to changes in the polarization state of light reflected from a surface, whereas the two ellipsometric parameters, $\tan\Psi$ (relative amplitude ratio) and Δ (relative phase shift), are recorded.[21] Via the basic equation of ellipsometry,

$$\tan(\Psi)\exp(i\Delta) = \frac{R_P}{R_S} = F(\Phi_0, \lambda, N_s, n_{amb}, n_j, k_j, d_j), \quad (1)$$

$\tan\Psi$ and Δ are correlated with the Fresnel reflection coefficients R_p (*p*-polarized electrical field) and R_s (*s*-polarized electrical field), which are complex functions of the angle of incidence Φ_0, the wavelength λ, the optical constants of the substrate (N_s), the ambient medium (n_{amb}), and the optical constants of surface layers (n_j, k_j) as well as their layer thick-

nesses d_j. Within the SE–QCM-D setup a spectroscopic ellipsometer with a rotating compensator (M-2000, J. A. Woollam Co., Inc., Lincoln, NE, USA) was used to measure tan Ψ and Δ of coated Au-crystals in the dry state and *in situ* at 396 wavelengths between 371 and 1679 nm with a fixed angle of incidence of $\Phi_0=65°$.

2. Quartz crystal microbalance with dissipation mode

In a quartz crystal microbalance, a mechanical oscillation is induced by an applied alternating current via the piezoelectric effect.[37] With the QCM-D setup, frequency shifts Δf and dissipation shifts ΔD that are due to additional surface layer and bulk solution effects (i.e., film adsorption or bulk viscosity change, respectively) can be measured at several overtones simultaneously. Here, for rigid films a linear dependency between Δf and the adsorbed surface density Γ is valid,[24] whereas for viscoelastic surface layers additional energy dissipation and a frequency (overtone)-dependent response have to be taken into account.[31] In describing the surface layer as a viscoelastic solid with a frequency-dependent complex shear modulus,

$$G = \mu_l + if\eta_l, \tag{2}$$

in the Voigt–Voinova representation,[26,27] Δf and ΔD can be assigned to a film with uniform thickness d_{visc}, density ρ_l, elastic shear (storage) modulus μ_l, and shear viscosity (loss modulus) η_l. Additionally the film deposited on the Au-coated electrode is assumed to be in contact with a Newtonian fluid under no-slip conditions.

An ellipsometry-compatible QCM-D module from Q-Sense was used (QELM 401, Q-Sense, Frölunda, Sweden) and installed on the ellipsometer base. The ellipsometry module consists of Teflon and titanium and is equipped with windows of quartz glass at an angle of incidence of 65°. The cell allows a small liquid volume above the crystal surface of 100 μl. Measurements were done in flow either with a constant flow rate of 0.4 ml/min or with stagnant solutions. The temperature was monitored over the whole experiment and held constant at 23 °C. For the exchange of liquids a syringe pump (NE-500 OEM, New Era Pump Systems, Inc., Farmingdale, NY, USA) was applied, increasing the flow gradually.

3. Course of experiments

Adsorption was performed at 1 mM salt concentration below the IEP of BSA [pH(IEP)=5.6 for defatted BSA (Ref. 38)] at pH 5.2 and above the IEP of the protein at pH 6. Protein adsorption was monitored for overall electrostatic attractive and repulsive conditions, respectively. Experiments were carried out by starting with the PAA brush in water and then exchanging the solution in constant flow at 0.4 ml/min to 1 mM buffer solution. Afterward, the solution was stagnant for 20 min and exchanged to 0.1 mg/ml protein solution by increasing the flow gradually until a constant flow (0.4 ml/min) was reached again, and the solution in the measurement chamber was exchanged after approximately 8 min. A volume of more than 10 ml protein solution was pumped through the cell with laminar flow above the brush-solution interface. Adsorption at constant flow conditions was monitored for 30 min at pH 5.2 (36.5 min at pH 6). When changes in the layer thickness d_{SE} grew smaller than 1 nm/min the protein solution was exchanged again to the pure buffer solution, and changes in the combined polymer-protein layer were monitored in the absence of protein in the solution. Finally, desorption was performed at pH 7.6 at increased electrostatic repulsive conditions. For the swelling experiments at higher salt content the PAA brush was also equilibrated in water, and the solution exchanged in constant flow at 0.4 ml/min to the buffer solution.

The effect of nonconstant flow conditions on swelling and protein adsorption was tested and was found to be marginal (<1%) for swelling and protein adsorption at electrostatic attractive conditions (pH < IEP$_{\mathrm{protein}}$). For protein adsorption at pH 6 (pH > IEP$_{\mathrm{protein}}$) the flow rate has an influence on the measurement. Thus, time periods of constant flow rate are marked in Fig. 4.

III. DATA MODELING

A. Spectroscopic ellipsometry data

For the PAA Guiselin brush, modeling of Δ and tan Ψ was done according to an optical box model consisting of the gold substrate, a PGMA, and a PAA layer. The dispersion of the gold substrate was fitted to a B-spline function and Δ-offsets of the windows determined before coating the crystal with PGMA and PAA. The thicknesses of the PGMA layer and the dry PAA layer (see above) were fitted using dispersion relations measured for thick bulk layers, with $n_{\mathrm{PGMA}}(631.5\ \mathrm{nm})=1.525$ and $n_{\mathrm{PAA}}(631.5\ \mathrm{nm})=1.522$. For the swollen PAA layer both thickness and refractive index could be modeled using a two parameter Cauchy relation for $n(\lambda)$.

The amount $\Gamma_{\mathrm{SE}}^{\mathrm{b}}$ of buffer solution in the swollen PAA layer was evaluated to be

$$\Gamma_{\mathrm{SE}}^{\mathrm{b}} = f_{\mathrm{b}}\rho_{\mathrm{b}}d_{\mathrm{PAA}}. \tag{3}$$

Here, f_{b} is the buffer fraction in the swollen PAA layer with a thickness d_{PAA}, which is modeled by a two component effective medium approach (EMA) according to Bruggeman, using the dispersion relation for dry PAA (component 1) and for the buffer solution (component 2).[39] The density of the buffer solution ρ_{b} was set to 1 $\mathrm{g/cm^3}$ due to the usage of low salt aqueous solutions. To allow comparison with the QCM-D data, changes $\Delta\Gamma_{\mathrm{SE}}^{\mathrm{b}}=\Gamma_{\mathrm{SE}}^{\mathrm{b}}-\Gamma_{\mathrm{SE}}^{\mathrm{w}}$ will be discussed, with $\Gamma_{\mathrm{SE}}^{\mathrm{w}}$ as the amount of water inside the box layer for the brush already swollen in water, calculated in the same manner as $\Gamma_{\mathrm{SE}}^{\mathrm{b}}$ [Eq. (3)].

For the *in situ* protein adsorption the box model was maintained, whereas instead for the PAA layer, thickness d_{comb} and refractive index n_{comb} for a combined PAA-BSA layer were modeled because protein can be assumed to penetrate into the PAA brush.[14] The amount of protein $\Gamma_{\mathrm{SE}}^{\mathrm{BSA}}$ was evaluated with a modified de Feijter approach:[23]

$$\Gamma_{SE}^{BSA} = d_{comb}\frac{n_{comb}-n_{amb}}{\left(\frac{dn}{dc}\right)_{comb}} - \Gamma_{PAA}, \quad (4)$$

$$\left(\frac{dn}{dc}\right)_{comb} = \frac{f_{BSA}(dn/dc)_{BSA} + f_{PAA}(dn/dc)_{PAA}}{f_{BSA}+f_{PAA}}. \quad (5)$$

Here, Γ_{SE}^{BSA} is obtained by subtracting the amount of the brush polymer Γ_{PAA} from the amount of the combined polymer-protein layer after adsorption, where $\Gamma_{PAA} = d_{PAA}(n_{PAA}-n_{amb})/(dn/dc)_{PAA}$ is also calculated by the de Feijter equation from the swollen brush layer thickness d_{PAA}, refractive index n_{PAA}, and the refractive index increment for PAA. The refractive index increment $(dn/dc)_{comb}$ of the combined polymer-protein layer is derived from the individual dn/dc values considering the volume fractions of polymer and protein, respectively. For BSA a refractive index increment of 0.187 was used,[23] and for PAA $dn/dc = 0.133$ was measured with a refractometer (Leica AR600, Leica Microsystems Inc., Buffalo NY, USA) at a wavelength of 589 nm. The volume fraction of polymer f_{PAA} in the combined polymer-protein layer was calculated as the product of the volume fraction of PAA in the swollen brush and the ratio of thicknesses d_{PAA}/d_{comb} of swollen brush and combined layer. This fraction f_{PAA} was fixed in a three component EMA model to derive the volume fraction f_{BSA} of the protein, with the buffer solution as the third component. In the EMA the effective dielectric function (refractive index n) of the heterogeneous layer is described on the basis of the known dispersion relations for n of the three components with varying individual volume fractions.[39] Here, the EMA according to Bruggeman was used, based on the assumption of random mixture and comparable volume fractions of f_{PAA}, f_{BSA}, and f_{buffer}. For BSA a fixed refractive index of $n = 1.575$ was used, obtained for BSA adsorption on gold surfaces.[40] To verify the modeling of the adsorbed amount, colorimetric quantification of the protein surface density for a similar adsorption experiment was performed and is included in the supplementary material.[41]

B. Quartz crystal microbalance data

Frequency and dissipation shifts for the odd overtones $j = 3, 5, \ldots, 11$ were measured with reference to the PAA brush already swollen in water. Δf_j and ΔD_j for the above overtones were fitted to a Voigt–Voinova model of one homogeneous viscoelastic layer,[26,27,31] using the software QTOOLS (Q-Sense, Frölunda, Sweden). For a fixed layer density ρ_l of 1 g/cm^3, changes in the viscoelastic thickness Δd_{visc} were evaluated, thus reflecting changes in the viscoelastically coupled amount $\Delta\Gamma_{QCMD}$ with respect to the brush in water:

$$\Delta\Gamma_{QCMD} = \rho_l \Delta d_{visc}. \quad (6)$$

For the evaluation of protein experiments $\Delta\Gamma_{QCMD}^{ads} = \Delta\Gamma_{QCMD} - \Delta\Gamma_{QCMD}^{b}$ was introduced, subtracting changes in the coupled buffer amount $\Delta\Gamma_{QCMD}^{b}$ due to the initial swelling in the buffer solution from the total amount of coupled molecules $\Delta\Gamma_{QCMD}$ upon protein adsorption. Thus, a direct comparison of changes in the viscoelastically coupled amount (buffer and protein molecules) in the adsorption process to the adsorbed amount of protein Γ_{SE}^{BSA} is possible, leading to quantitative information on the changes in coupled buffer molecules $\Delta\Gamma_{buffer}^{ads} = \Delta\Gamma_{QCMD}^{ads} - \Gamma_{SE}^{BSA}$ in the adsorption and desorption of protein. The density and viscosity of the buffer solutions were set to the values known for water. Additionally, for the protein adsorption experiments, changes in the shear viscosity of the combined polymer-protein film were evaluated independently from Δd_{visc}, as given by the Voigt–Voinova model.

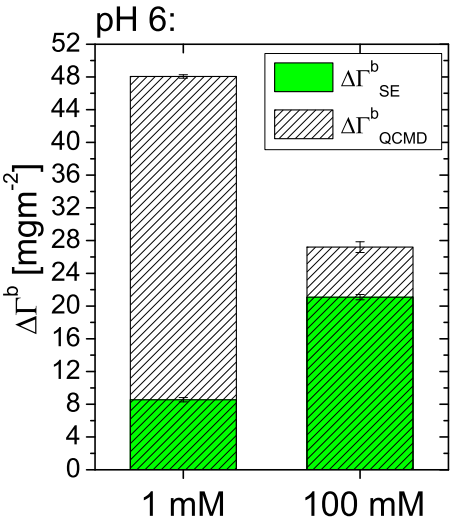

FIG. 1. (Color online) Increase in the viscoelastically coupled amount derived from QCM-D and in the buffer amount inside the brush derived from SE for swelling at *p*H 6 in 1 and 100 mM buffer solutions. All values are referenced to the brush already swollen in water.

IV. RESULTS AND DISCUSSION

A. Swelling dependent on ionic strength

With the hybrid technique of QCM-D and SE, changes in the amount of buffer solution inside the brush layer ($\Delta\Gamma_{SE}^{b}$) and totally coupled to the brush-solution interface ($\Delta\Gamma_{QCMD}^{b}$) can be addressed simultaneously. For the swelling of PAA Guiselin brushes in 1 and 100 mM buffer solutions at *p*H 6 these buffer amounts are displayed in Fig. 1. For this special type of polymer brush it was shown previously that the dissociation behavior of COOH-groups is similar to end-grafted PAA brushes.[11]

A large difference between the amount $\Delta\Gamma_{SE}^{b}$ inside the SE-box layer and $\Delta\Gamma_{QCMD}^{b}$ is visible at 1 mM salt concentration. One explanation for this behavior could be the increased contrast of the acoustic QCM-D method.[33] Single PAA chains are suspected to protrude into the buffer solution to a higher extent than indicated by the thickness of the swollen brush modeled from SE measurements, and QCM was discussed to be sensitive to these dilute regions of the polymer segment density profile. Another reason could be changes in the electrical double layer due to a different counterion and coion density at the brush-solution interface in 1 mM buffer solution compared to water. When more ions

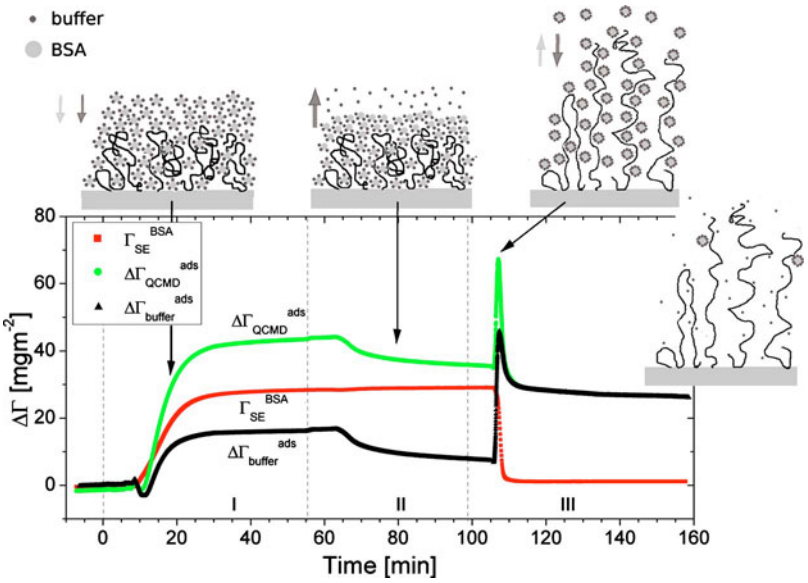

FIG. 2. (Color online) Adsorbed amount of protein Γ_{SE}^{BSA}, changes in the total amount viscoelastically coupled to the brush surface $\Delta\Gamma_{QCMD}^{ads}$, and changes in the amount of coupled buffer components $\Delta\Gamma_{buffer}^{ads}$. For clearer presentation measurements are referenced to the brush surface in buffer solution, displaying (I) adsorption in 0.1 mg/ml protein solution at *p*H 5.2, (II) desorption in 1 mM buffer solution at *p*H 5.2, and (III) desorption in 1 mM buffer solution at *p*H 7.6. Dotted lines indicate starting times of the pump for the exchange of solution. Corresponding frequency shifts and dissipation values can be found in the supplementary material (Ref. 41).

couple to the vibration of the surface in the buffer solution, Δf decreases and ΔD increases, indicating a higher viscoelastic thickness of the brush layer.

Upon swelling in 100 mM buffer solution a decrease in $\Delta\Gamma_{QCMD}^{b}$ is observed compared to swelling in 1 mM solution, although the swollen brush thickness d_{PAA} is higher at 100 mM (d_{PAA}=50 nm), and thus the amount of buffer inside this box layer is increased compared to swelling in 1 mM (d_{PAA}=35 nm). This observation favors an influence of the ion concentration at the brush-solution interface on the difference between $\Delta\Gamma_{QCMD}^{b}$ and $\Delta\Gamma_{SE}^{b}$. The amount of ions at the interface is assumed to decrease with increasing salt content due to a better screening of charges in the brush layer by counterions. The roughness of the swollen brush surface on the other hand is expected to increase with increasing swollen brush thickness. Furthermore the optical contrast should decrease because of a decreasing refractive index difference between brush layer and aqueous solution, leading to an underestimation of the thickness by ellipsometry. If dangling polymers not considered by the ellipsometric box model would contribute significantly to the differences between $\Delta\Gamma_{QCMD}^{b}$ and $\Delta\Gamma_{SE}^{b}$, an increase of $\Delta\Gamma_{QCMD}^{b} - \Delta\Gamma_{SE}^{b}$ would be expected, contrary to the observed results. Hence, we could show that changes in the ion concentration and distribution at the brush surface are dominating the differences between buffer amount in the SE-model layer and the viscoelastically coupled buffer, and that this hybrid technique provides an access to the combined amount of ions and water coupled to an interface. The same experiments performed at *p*H 5.2 can be found in the supplementary material.[41]

B. BSA adsorption below the IEP of the protein

In Fig. 2 the adsorbed amount of protein Γ_{SE}^{BSA} derived from SE measurements, changes in the amount of protein and buffer molecules $\Delta\Gamma_{QCMD}^{ads}$ viscoelastically coupled to the brush surface, and changes in the coupled buffer amount $\Delta\Gamma_{buffer}^{ads}$ are displayed, starting with adsorption in 0.1 mg/ml protein solution at *p*H 5.2 (I), desorption in the corresponding buffer solution at *p*H 5.2 (II), and desorption in 1 mM buffer solution at *p*H 7.6 (III). Since $\Delta\Gamma_{QCMD}^{ads}$ is referenced to the brush swollen in the buffer, negative $\Delta\Gamma_{QCMD}^{ads}$ implies a reduction of the viscoelastically coupled amount compared to the brush in 1 mM buffer solution. For a better understanding schemes of the brush surfaces are added for each step of the experiment. The transport processes, as indicated by the measurement data, are marked with arrows, light gray for BSA and dark gray for water molecules and ions combined.

In field I of Fig. 2 a different rate of increase for Γ_{SE}^{BSA} and $\Delta\Gamma_{QCMD}^{ads}$ can be observed. In fact $\Delta\Gamma_{QCMD}^{ads}$ first decreases before it increases again considerably faster than Γ_{SE}^{BSA}. Since the SE data are evaluated according to De Feijter *et al.*,[23] solely the increase of the adsorbed amount of protein is monitored, making the observation highly interesting. In $\Delta\Gamma_{QCMD}^{ads}$ both the increase of the coupled amount of protein and changes in the coupled amount of buffer components are reflected. Thus, to the best of our knowledge, differences between $\Delta\Gamma_{QCMD}^{ads}$ and Γ_{SE}^{BSA} reflect changes in the viscoelastically coupled amount of counterions and coions as well as water molecules.

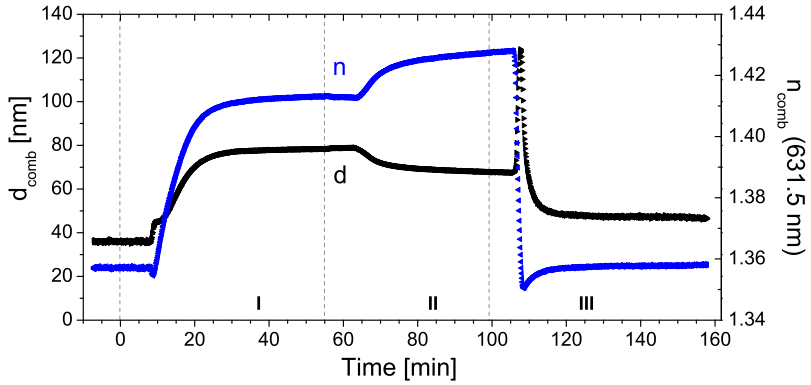

FIG. 3. (Color online) Total refractive index $n_{comb}(\lambda=631.5\ \text{nm})$ and combined polymer-protein layer thickness d_{comb}, corresponding to the measurements presented in Fig. 2.

Here, a small increase of $\Delta\Gamma_{buffer}^{ads}$ between 7.5 and 9 min followed by a noticeable decrease from 9 to 11 min is visible. We refer this feature to the exchange of solution in the measurement chamber. However, the decrease in $\Delta\Gamma_{buffer}^{ads}$ from 9 to 11 min indicates a removal of viscoelastically coupled molecules from the surface, possibly due to the exchange of coupled buffer components to protein molecules. The subsequent increase in $\Delta\Gamma_{QCMD}^{ads}$ with a higher rate than observed for Γ_{SE}^{BSA} can be well understood considering the absorption of hydrated protein molecules with a surrounding electrical double layer to the brush surface. Here, the amount of buffer molecules coupling to the surface in the adsorption process is $16\pm1\ \text{mg/m}^2$ compared to the pure brush in 1 mM buffer solution.

Interestingly when exchanging the solution to 1 mM buffer solution again (field II), although the amount of protein at the surface (Γ_{SE}^{BSA}) stays constant, $\Delta\Gamma_{QCMD}^{ads}$ decreases. Thus, ions and water molecules are released from the surface.

The decrease in $\Delta\Gamma_{buffer}^{ads}$ is accompanied by an increase in the total refractive index and a decrease in the combined polymer-protein layer thickness (Fig. 3), indicating a contraction of this polymer-protein layer within this box-model picture. But also a sharpening of the polymer-protein-solution interface could possibly lead to these results for n and d.

Finally, a high fraction of BSA is desorbed in exchanging the 1 mM solution at *p*H 5.2 to a 1 mM solution at *p*H 7.6 (field III). The desorption process can be monitored, where upon the decrease in Γ_{SE}^{BSA} first a significant increase in $\Delta\Gamma_{QCMD}^{ads}$ and thus in $\Delta\Gamma_{buffer}^{ads}$ occurs. This behavior can be explained by an additional coupling of buffer molecules in the desorption process due to a temporarily strong stretching of the polymer-protein layer before protein molecules start to desorb. This stretching can also be found from the sharp increase in d_{comb} (Fig. 3) that accompanies the increase in $\Delta\Gamma_{QCMD}^{ads}$. It is also noted that after desorption of the protein, $\Delta\Gamma_{QCMD}^{ads}$ remains at a relatively high value at $26.4\ \text{mg/m}^2$, influenced not only by the increased dissociation of COOH-groups at higher *p*H, but also by the remaining small BSA fraction of $1.6\ \text{mg/m}^2$. We refer the latter to as irreversible structural changes in the BSA molecules at the PAA brush surface, as observed, for example, in BSA adsorption at silica surfaces.[42]

C. BSA adsorption above the IEP of the protein

The adsorption experiment was repeated in the same way at *p*H 6 to determine changes in the amount of coupled buffer components upon adsorption at the wrong side of the IEP of BSA (*p*H 5.6), and in Fig. 4 changes in Γ_{SE}^{BSA}, $\Delta\Gamma_{QCMD}^{ads}$, and $\Delta\Gamma_{buffer}^{ads}$ are displayed.

In field I $\Delta\Gamma_{QCMD}^{ads}$ again increases more rapidly than Γ_{SE}^{BSA}. Here, over a range of 5 min (9 min after starting the exchange of buffer solution) an increase in $\Delta\Gamma_{buffer}^{ads}$ up to $8\pm1\ \text{mg/m}^2$ can be observed that decreases again to $5.5\pm0.4\ \text{mg/m}^2$ and stays constant in the adsorption process. Thus, an excess amount of buffer components is coupled to the brush surface at the beginning of protein adsorption at the wrong side of the IEP, which equilibrates during the adsorption process. Here, the peak in $\Delta\Gamma_{buffer}^{ads}$ at 14 min is reflected as a negative peak in the refractive index n_{comb}(631.5 nm), whereas the combined polymer-protein layer thickness d_{comb} is still increasing (Fig. 5). After 40 min d_{comb} stays virtually constant, but n_{comb}(631.5 nm) is further increasing until the end of the adsorption experiment and exchange of the protein solution to pure buffer solution. These findings can be interpreted as a densification of the combined protein-polymer layer in the ongoing adsorption process, now in stagnant solution after 36.5 min of the experiment. Thus, protein is continuously incorporated into the combined layer.

After exchange of the protein solution to buffer solution both $\Delta\Gamma_{QCMD}^{ads}$ and Γ_{SE}^{BSA} decrease in field II and protein desorption takes place, whereas the decrease in $\Delta\Gamma_{QCMD}^{ads}$ is faster, indicating desorption of buffer components alongside the protein, as it is expected when the hydration shell of protein molecules is taken into account. The desorption process in pure 1 mM buffer at *p*H 6 is accompanied by a decrease in both thickness d_{comb} and refractive index n_{comb} in Fig. 5. At this *p*H desorption of protein begins with starting the pump for the exchange of solution at 158 min of the

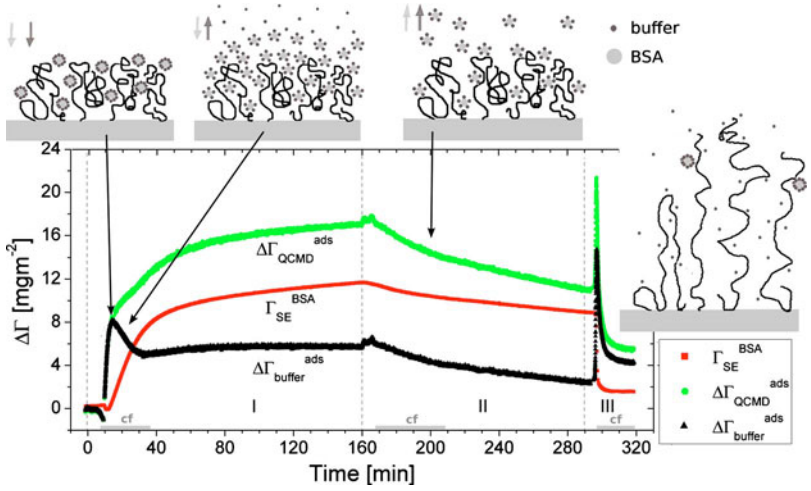

FIG. 4. (Color online) Adsorbed amount of protein Γ_{SE}^{BSA}, changes in the amount viscoelastically coupled to the brush surface $\Delta\Gamma_{QCMD}^{ads}$, and changes in the amount of coupled buffer components $\Delta\Gamma_{buffer}^{ads}$. For clearer presentation measurements are referenced to the brush surface in buffer solution, displaying (I) adsorption in 0.1 mg/ml protein solution at *p*H 6, (II) desorption in 1 mM buffer solution at *p*H 6, and (III) desorption in 1 mM buffer solution at *p*H 7.6. Dotted lines indicate starting times of the pump for the exchange of solution, and time periods of constant flow conditions (cf. gray bar) are marked. Corresponding frequency shifts and dissipation values can be found in the supplementary material (Ref. 41).

experiment, indicating a high sensitivity of the combined polymer-protein surface on shear forces/flow for this *p*H at the wrong side of the IEP of BSA.

When exchanging the buffer to 1 mM at *p*H 7.6 the same desorption features as observed in the adsorption experiment at *p*H 5.2 (Fig. 2) are visible, but less pronounced. Also a temporarily stretching of the layer, indicated by a change in the combined layer thickness d_{comb} from 69 to 90 nm, takes place, whereas the increase is also smaller than at *p*H 5.2, where a stretching from 68 to 124 nm could be observed. These differences are due to less protein adsorbed at *p*H 6 than at *p*H 5.2. Therefore, fewer charged protein molecules contribute to the incorporation of additional buffer components and thus the stretching of the layer in the desorption process. A similar remaining adsorbed amount of protein of 1.7 mg/m^2 as after adsorption at *p*H 5.2 and desorption at *p*H 7.6 can be observed. Thus, also upon adsorption at the wrong side of the IEP of BSA irreversible denaturation of the protein is most likely to take place.

D. Changes in the shear viscosity during the adsorption process

Changes in the shear viscosity $\Delta\eta_l$ upon BSA adsorption in 1 mM buffer solution are displayed in Fig. 6 for adsorption at *p*H 5.2 [Fig. 6(a)] and at *p*H 6 [Fig. 6(b)] as discussed in the previous two subsections. Here, for adsorption at *p*H 5.2 an increase in $\Delta\eta_l$ over one order of magnitude occurs upon adsorption (field I). Thus, the internal friction in the combined polymer-protein layer is considerably higher than for the bare brush surface. When exchanging the protein solution to 1 mM buffer solution again, a further increase in the shear viscosity is monitored (field II), which is interesting because the amount of ions and water molecules was shown to decrease in Fig. 2. Thus, the less hydrated protein-brush layer in field II has a higher viscosity at the present environmental conditions than the more hydrated protein-brush layer in equilibrium with 0.1 mg/ml protein concentration in the same 1 mM buffer solution (field I). With desorption of the

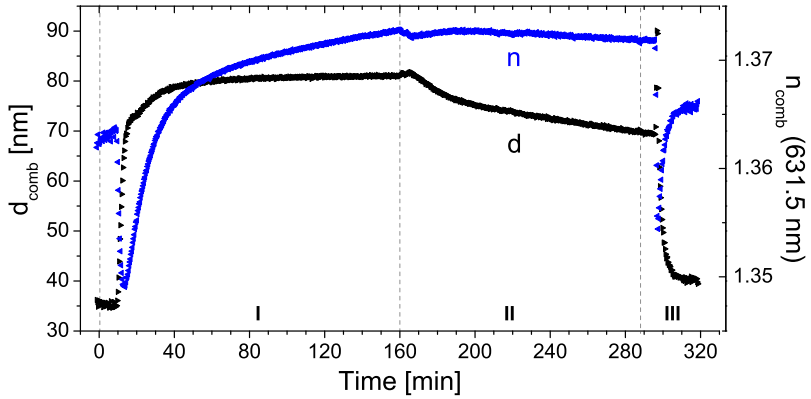

FIG. 5. (Color online) Total refractive index $n_{comb}(\lambda=631.5$ nm) and combined polymer-protein layer thickness d_{comb}, corresponding to the measurements presented in Fig. 4.

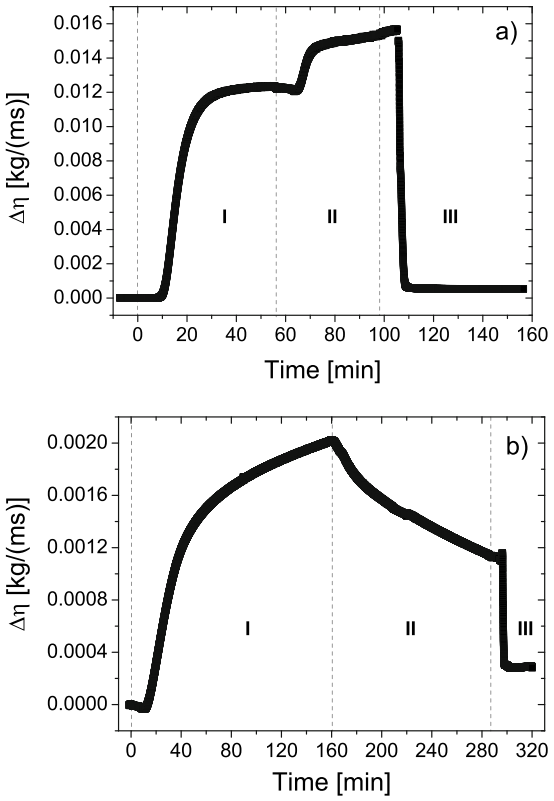

FIG. 6. Changes in the viscosity $\Delta\eta_l$ upon BSA adsorption in 1 mM salted solution at (a) *p*H 5.2 and (b) *p*H 6. Measurements are referenced for clearer presentation to the brush surface in buffer solution, displaying (I) adsorption in 0.1 mg/ml protein solution, (II) desorption in 1 mM buffer solution, and (III) desorption in 1 mM buffer solution at *p*H 7.6.

protein in field III at *p*H 7.6, $\Delta\eta_l$ decreases to values comparable with the pure brush surface, underlining the importance of the protein on the surface for a high shear viscosity.

At *p*H 6 the change in the shear viscosity upon protein adsorption is relatively small, only 0.002 kg/(m s) (field I), compared to the changes observed at *p*H 5.2. Here, at the latter *p*H a six times higher $\Delta\eta_l$ was observed, whereas the adsorbed amount of protein at *p*H 5.2 was 2.3 times higher than at *p*H 6. The desorption of protein upon exchange to the buffer solution at *p*H 6 is reflected again in $\Delta\eta_l$, which is decreasing with decreasing amount of protein at the brush surface (field II). Finally, after desorption at *p*H 7.6 the remaining changes in the shear viscosity are similar to $\Delta\eta_l$ after the adsorption experiment at *p*H 5.2 (field III). Thus, similar brush states are achieved at *p*H 7.6 after adsorption experiments at overall electrostatic attractive and repulsive conditions at this low salt content in solution, considering thickness d_{comb}, remaining amount Γ_{SE}^{BSA}, viscoelastically coupled amount $\Delta\Gamma_{QCMD}^{ads}$, and remaining change in the shear viscosity $\Delta\eta_l$.

V. SUMMARY AND CONCLUSIONS

In simultaneous SE–QCM-D studies changes in the amount of coupled buffer in swelling and protein adsorption experiments could be obtained quantitatively, monitoring in real time hydration as well as incorporation of counterions and coions. Thus, the interaction of solvent and adsorbate molecules with the surface can be addressed separately, indicating not only the potential of these simultaneous measurements for the quantitative investigation of molecules involved in adsorption, but also replacement processes or specific interactions at biointerphases.

Here, for PAA Guiselin brushes a considerable increase in the amount of viscoelastically coupled buffer components could be observed upon swelling in electrolyte solutions. Compared to the buffer content inside the swollen brush layer as given by a SE-box model, a high amount was coupled to the brush-solution interface at low salt concentration. Here, the decrease of coupled buffer amount with increasing salt content indicates high influence of the ion concentration at the brush-solution interface (electrical double layer) on the difference between optically (SE) and acoustically (QCM-D) determined buffer amounts at the brush surface.

For BSA adsorption at these PAA Guiselin brushes, the rate of increase of the viscoelastically coupled amount was higher than the increase of amount of protein at the surface for both adsorption experiments at overall electrostatic attractive (*p*H 5.2) and overall electrostatic repulsive (*p*H 6) conditions. Thus, the incorporation of buffer molecules into the protein-brush layer during the adsorption process was investigated quantitatively, providing further insight into the adsorption of the model protein BSA at flexible polyelectrolyte surfaces.

Especially interesting is adsorption at *p*H 6 at the wrong side of the IEP of the protein. Here, a coupling of an excess amount of buffer components could be observed. Thus, viscoelastically coupled buffer molecules are released from the surface in the ongoing adsorption process, indicating an adjustment of charges and possibly also charge distribution in the combined polymer-protein layer.

Regarding the desorption of protein at *p*H 7.6 from both brush surfaces at overall electrostatic attractive and repulsive conditions, an increase in the polymer-protein combined layer thickness accompanied by a strong increase in the viscoelastically coupled amount was found. We interpret these findings as a stretching of the combined brush-protein layer with additional incorporation of buffer molecules in the desorption process before desorption of protein molecules actually takes place.

Finally, the shear viscosity and thus the internal friction of the brush-protein layer were one order of magnitude higher upon electrostatic attractive adsorption at *p*H 5.2 than upon adsorption at the wrong side of the IEP of the protein, which we refer to the high amount of protein in the combined polymer-protein layer at *p*H 5.2. Hence, we show that by incorporation of protein the internal friction of a highly swellable polymer surface coating can be increased considerably, highly interesting for surfaces in flowing biological fluids.

ACKNOWLEDGMENTS

We gratefully acknowledge financial support from the German Science Foundation (DFG Project Nos. Sta 324/28-1

and Ei 317/5-1), The Procter & Gamble Company, the J. A. Woollam Company, Inc., Nebraska NSF-EPSCoR, and the University of Nebraska–Lincoln College of Engineering.

[1]T. P. Russell, Science **297**, 964 (2002).
[2]M. A. Cohen Stuart, W. T. S. Huck, J. Genzer, M. Müller, C. Ober, M. Stamm, G. B. Sukhorukov, I. Szleifer, V. V. Tsukruk, M. Urban, F. Winnik, S. Zauscher, I. Luzinov, and S. Minko, Nature Mater. **9**, 101 (2010).
[3]P. Uhlmann, L. Ionov, N. Houbenov, M. Nitschke, K. Grundke, M. Motornov, S. Minko, and M. Stamm, Prog. Org. Coat. **55**, 168 (2006).
[4]R. Toomey and M. Tirrell, Annu. Rev. Phys. Chem. **59**, 493 (2008).
[5]W. J. Brittain and S. Minko, J. Polym. Sci., Part A: Polym. Chem. **45**, 3505 (2007).
[6]F. Zhou and W. T. S. Huck, Phys. Chem. Chem. Phys. **8**, 3815 (2006).
[7]E. P. K. Currie, W. Norde, and M. A. Cohen Stuart, Adv. Colloid Interface Sci. **100–102**, 205 (2003).
[8]E. P. K. Currie, A. B. Sieval, G. J. Fleer, and M. A. Cohen Stuart, Langmuir **16**, 8324 (2000).
[9]S. S. Dukhin, R. Zimmermann, and C. Werner, J. Phys. Chem. B **111**, 979 (2007).
[10]X. Guo and M. Ballauff, Phys. Rev. E **64**, 051406 (2001).
[11]D. Aulich, O. Hoy, I. Luzinov, M. Brücher, R. Hergenröder, E. Bittrich, K.-J. Eichhorn, P. Uhlmann, M. Stamm, N. Esser, and K. Hinrichs, Langmuir **26**, 12926 (2010).
[12]M. Ballauff and O. Borisov, Curr. Opin. Colloid Interface Sci. **11**, 316 (2006).
[13]H. Zhang and J. Rühe, Macromolecules **38**, 4855 (2005).
[14]S. Rosenfeldt, A. Wittemann, M. Ballauff, E. Breininger, J. Bolze, and M. Dingenouts, Phys. Rev. E **70**, 061403 (2004).
[15]P. M. Biesheuvel, F. A. M. Leermakers, and M. A. Cohen Stuart, Phys. Rev. E **73**, 011802 (2006).
[16]O. Hollmann, T. Gutberlet, and C. Czeslik, Langmuir **23**, 1347 (2007).
[17]W. M. de Vos, P. M. Biesheuvel, A. de Keizer, J. M. Kleijn, and M. A. Cohen Stuart, Langmuir **24**, 6575 (2008).
[18]W. M. de Vos, F. A. M. Leermakers, A. de Keizer, M. A. Cohen Stuart, and J. M. Kleijn, Langmuir **26**, 249 (2010).
[19]K. Henzler, B. Haupt, K. Lauterbach, A. Wittemann, O. Borisov, and M. Ballauff, J. Am. Chem. Soc. **132**, 3159 (2010).
[20]E. Bittrich, M. Kuntzsch, K.-J. Eichhorn, and P. Uhlmann, J. Polym. Sci., Part B: Polym. Phys. **48**, 1606 (2010).
[21]C. Werner, K.-J. Eichhorn, K. Grundke, F. Simon, W. Grählert, and H.-J. Jacobasch, Colloids Surf., A **156**, 3 (1999).
[22]S. Reichelt, K.-J. Eichhorn, D. Aulich, K. Hinrichs, N. Jain, D. Appelhans, and B. Voit, Colloids Surf., B **69**, 169 (2009).
[23]J. A. de Feijter, J. Benjamins, and F. A. Veer, Biopolymers **17**, 1759 (1978).
[24]G. Sauerbrey, Z. Phys. **155**, 206 (1959).
[25]M. Rodahl, F. Höök, A. Krozer, P. Brzezinski, and B. Kasemo, Rev. Sci. Instrum. **66**, 3924 (1995).
[26]M. V. Voinova, M. Jonson, and B. Kasemo, J. Phys.: Condens. Matter **9**, 7799 (1997).
[27]M. V. Voinova, M. Jonson, and B. Kasemo, Biosens. Bioelectron. **17**, 835 (2002).
[28]H.-S. Lee and L. S. Penn, Macromolecules **41**, 8124 (2008).
[29]M. Kaufmann, Y. Jia, L. Renner, S. Gupta, D. Kuckling, C. Werner, and T. Pompe, Soft Matter **6**, 937 (2010).
[30]M. V. Gormally, R. K. McKibben, M. S. Johal, and C. R. D. Selassie, Langmuir **25**, 10014 (2009).
[31]F. Höök, B. Kasemo, T. Nylander, C. Fant, K. Scott, and H. Elwing, Anal. Chem. **73**, 5796 (2001).
[32]K. B. Rodenhausen, M. Guericke, A. Sarkard, T. Hofmann, N. Ianno, M. Schubert, T. E. Tiwald, M. Solinsky, and M. Wagner, "Virtual separation approach to study porous ultra-thin films by combined spectroscopic ellipsometry and quartz crystal microbalance methods," Thin Solid Films (in press).
[33]A. Domack, O. Prucker, J. Rühe, and D. Johannsmann, Phys. Rev. E **56**, 680 (1997).
[34]T. J. Halthur and U. M. Elofsson, Langmuir **20**, 1739 (2004).
[35]M. Aubouy, O. Guiselin, and E. Raphael, Macromolecules **29**, 7261 (1996).
[36]E. Bittrich, D. Aulich, K.-J. Eichhorn, K. Hinrichs, P. Uhlmann, I. Luzinov, and M. Stamm, Polym. Mater. Sci. Eng. **101**, 930 (2009).
[37]D. A. Buttry and M. D. Ward, Chem. Rev. (Washington, D.C.) **92**, 1355 (1992).
[38]F. Soetewey, M. Rosseneu-Motreff, R. Lamote, and H. Peeters, J. Biochem. (Tokyo) **71**, 705 (1972).
[39]D. E. Aspnes, Thin Solid Films **89**, 249 (1982).
[40]H. Arwin, Appl. Spectrosc. **40**, 313 (1986).
[41]See supplementary material at http://dx.doi.org/10.1116/1.3530841 for a comparison of the adsorbed protein amount as derived by using the de Feitjer equation with an alternative approach based on a colorimetric assay. Additionally the influence of ionic strength of the buffer at pH=5.2 on swelling of the brush is shown, and the frequency and dissipation shifts of the protein adsorption experiments are displayed.
[42]L. Lensun, T. A. Smith, and M. L. Gee, Langmuir **18**, 9924 (2002).